

Impact of nonlinear friction on frequency response function measurements

V. Lampaert, J. Swevers, F. Al-Bender

Department of Mechanical Engineering, division PMA, K.U.Leuven, Belgium

e-mail : vincent.lampaert@mech.kuleuven.ac.be

Abstract

This paper discusses the impact of nonlinear friction on frequency response function (FRF) measurements of mechanical systems with nonlinear friction. Having an idea of the level of nonlinear distortion is valuable information for robust linear control design: it allows to estimate the level of accuracy of a linear approximation of the system under consideration. The impact of nonlinear distortions is measured using the multisine excitation approach presented in [5]. A linear approximation of the system and a reliable estimate of the level of systematic and stochastic nonlinear distortions are derived using a single special odd multisine excitation. This is shown by means of simulations of mechanical system with friction. The friction model is nonlinear and integrates sliding and presliding behaviour [7].

1 Introduction

The goal of this paper is to provide the reader insight in the behaviour of friction as a nonlinear distortion and its impact on FRF measurements. In order to formalize the discussion, we use the general structure given in figure 1.

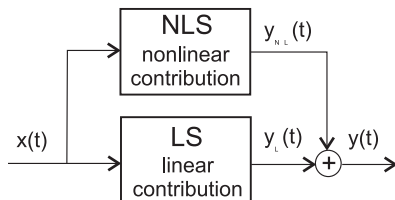


Figure 1: *General structure*

The measured output consists of a linear y_L and a nonlinear y_{NL} contribution. For simplicity we assume that the linear contribution dominates over the nonlinear one. Under this assumption we have two basic options:

- 1) the goal of the measurement is to get the FRF of the underlying linear system, minimizing the impact of the nonlinear system (NLS) on the measurements;
- 2) try to find the best linear approximation to the global system, including the NLS for the considered class of excitations.

The first option is the best choice if some underlying linear physical model exists and the user wishes to identify it as good as possible.

The second choice is preferred if the model is to

be used to describe the relation between input and output using linear models, e.g. in robust linear control design. At that moment, the nonlinearity can be linearized around the operation point of the test. The best linear approximation is called the related linear dynamic system (RLDS).

Section 2 describes a novel integrated friction model which will be used in the simulation setup described in section 4. Section 3 describes the properties of FRF measurements in the presence of nonlinear distortions. Three types of random multisine excitations are used: odd, odd-odd and special odd multisine. The results of these experiments on the simulation setup are discussed in section 5. The considered mechanical system has no even nonlinearities and the special odd excitation gives us a measure for the impact of odd nonlinearities on the FRF measurement even if only data from one experiment is available.

2 Nonlinear friction model

Swevers et al. [7] describes a novel integrated friction model. This section briefly summarizes the results. This model will be used in section 4 to simulate the nonlinear friction forces.

2.1 Different friction regimes

In building up an elaborate friction model structure, one begins by distinguishing two different friction

regimes: the presliding regime and the sliding regime.

1) In the presliding regime or the micro-slip regime the adhesive forces (at asperity contacts) are dominant such that the friction force appears to be a function of displacement rather than the velocity. This is so because asperity junctions deform elasto-plastically (depending on their individual loading) thus behaving like nonlinear springs. As the displacement increases more and more junctions will break resulting eventually in sliding (second regime below). This “break-away” displacement may depend on diverse characteristics of the contact and surface texture: topography, hardness, surface layer metallurgy, etc.

2) In the sliding regime all asperity junctions have broken apart (alternatively, all asperity contacts) such that the friction force is now a more pronounced function of sliding velocity, due to e.g. the build up of lubricating films.

The transition between these two regimes must not be considered as a sudden discontinuity in the friction process, since there is a build up in micro-slip leading to sliding. Therefore using a switching function to choose one of the regimes is physically not justified. It is better to integrate the two regimes into one continuous model.

2.2 Mathematical description

The LuGre model [2] describes friction in sliding and presliding by one differential equation and one output equation. The shortcomings of this model lies in the inadequacy of the hysteresis part since (i) it does not account for nonlocal memory [4], and (ii) it can not accommodate arbitrary displacement-force transition curves. The friction model proposed by [7] overcomes this problem.

The friction force F_f is modelled by a set of two equations which depend on a state variable z representing the average deformation of the asperity junctions:

1) The **friction force equation** yields the friction force based on the current hysteresis transition curve, the derivative of the state variable z and the current velocity:

$$F_f = F_h(z) + \sigma_1 \frac{dz}{dt} + \sigma_2 v. \quad (1)$$

σ_1 is a micro-viscous damping coefficient, σ_2 is the viscous damping coefficient, v is the relative velocity between the mass and the ground. $F_h(z)$ is the hysteresis friction force, i.e. the part of the friction force

exhibiting hysteretic behaviour. It is a static hysteresis nonlinearity with nonlocal memory [4]. That is to say that it is a multi-branch nonlinear function for which:

- (i) branch-to-branch transitions occur after velocity reversals,
- (ii) the branches (transition curves) are determined only by the past extremum values of F_h , i.e. are independent of the particular manner of the variation of z between extremum points,
- (iii) the future values of F_h past any time instant t_0 not only depend on the value of F_h at t_0 and the values of z at all subsequent instants of time $t \geq t_0$, but also on past extremum values of F_h .

This last property is in contrast to the behaviour of hysteresis nonlinearities with *local* memory, where the past exerts its influence upon the future through the current value of the output only [4].

2) The **nonlinear state equation** is based on the current hysteresis transition curve and the current velocity:

$$\frac{dz}{dt} = v(1 - \text{sign} \left(\frac{F_h(z)}{s(v)} \right) * \left| \frac{F_h(z)}{s(v)} \right|^n) \quad (2)$$

$s(v)$ models the constant velocity behaviour in sliding. The parameter n allows to modify the influence of $\frac{F_h(z)}{s(v)}$ on the difference between $\frac{dz}{dt}$ and v , such that the model behaviour corresponds better to friction measurements in the transition from presliding to sliding. For example, for high positive values of n , $\frac{dz}{dt}$ will be different from v only when $F_h(z)$ is close to $s(v)$.

The following sections describe the characteristics of the model for two steady-state solutions: one in sliding (constant velocity) and one in presliding (zero velocity). The constant velocity behaviour is similar to the behaviour of the LuGre model. The presliding behaviour is an improvement on the LuGre model due to the inclusion of a hysteresis model with nonlocal memory and the modelling of the hysteresis transition curves.

2.2.1 Constant velocity behaviour

For constant velocity, different from zero, and in steady state ($\frac{dz}{dt} = 0$), the state equation (2) reduces to:

$$F_h = s(v).$$

The friction force equation (1) reduces to :

$$F_f = F_h(z) + \sigma_2 v = s(v) + \sigma_2 v.$$

The function $s(v)$ determines the constant velocity characteristics in the sliding regime near zero velocity while $\sigma_2 v$ becomes significant at high velocity. Choosing:

$$s(v) = F_c + (F_s - F_c) * e^{-\left(\frac{v}{v_s}\right)^\delta}, \quad (3)$$

with F_c the Coulomb friction, F_s the static friction, v_s the Stribeck velocity and δ an arbitrary exponent, yields the classical Stribeck effect.

2.2.2 Zero velocity behaviour

For zero velocity, which corresponds to steady-state in presliding, equations (1) and (2) reduce to:

$$\begin{aligned} F_f &= F_h(z) \\ \frac{dz}{dt} &= 0. \end{aligned}$$

In the presliding regime the hysteresis force dominates in the friction force.

2.3 Properties of the model

With this model it is possible to describe accurately friction behaviour as observed in experiments or described in literature: (i) Stribeck effect in sliding, (ii) hysteretic behaviour in presliding, (iii) friction lag, (iv) varying break-away and (v) stick-slip behaviour. An elaborate description of the properties and a possible implementation of the hysteresis force F_h is given in [7].

3 Properties of FRF measurements in the presence of nonlinear distortions

This section considers the behaviour of nonlinear systems (NLS) for random multisine excitations. This is a periodic random excitation with a user defined choice for the amplitude spectrum. Schoukens et al. [5] show that the nonlinear distortions split in two classes: systematic and stochastic contributions.

- *systematic contributions*: there exists a related linear dynamic system (RLDS) to which the expected value of the FRF estimate converges under weak conditions. This RLDS is also linked

to the classical results where the system is excited with normally distributed noise. It differs from the underlying linear system G_0 by the systematic contributions of the nonlinear distortions G_B .

- *stochastic contributions*: even for a wide range of frequencies, the FRF estimate is not smooth as a function of the frequency. It is scattered around its expected value and these deviations do not converge to zero. They are called the stochastic nonlinear distortions (SNLS).

So the measured FRF can be written as the sum of 3 parts:

$$G(j\omega) = G_R(j\omega) + G_S(j\omega) + N_G(j\omega), \quad (4)$$

with $G_R(j\omega)$ the related dynamic system (RLDS), $G_S(j\omega)$ the stochastic nonlinear contributions (SNLS), and $N_G(j\omega)$ the errors due to the output noise. $G_R(j\omega)$ consists, in turn, of two parts:

$$G_R(j\omega) = G_0(j\omega) + G_B(j\omega), \quad (5)$$

with $G_0(j\omega)$ the underlying linear system and $G_B(j\omega)$ the bias or systematic errors due to the nonlinear distortions. $G_S(j\omega)$ is called a stochastic contribution since it behaves as uncorrelated noise (over the frequencies) although the reader should be aware that it is not a noise component. Due to this noisy behaviour, the presence of nonlinear distortions is often not recognized.

When a nonlinear system is described by a linear system, it is important to be sure that the best linear approximation is made. This is actually the case for G_R (which is therefore also called the best linear approximation). This follows immediately from the fact that $G_R(j\omega) = E[Y(j\omega)/U(j\omega)]$, with U and Y the DFT of the input and output signal, can also be written as $G_R(j\omega) = S_{YX}(j\omega)/S_{UU}(j\omega)$ with S_{YU} the cross-spectrum and S_{UU} the input autospectrum. It is shown that this estimate is the best linear approximation in least square sense [3, 1]. The estimated impulse response (and the corresponding FRF) minimizes the mean square value of the difference between the measured and the predicted output over the measurement interval. The reader should be aware that the best linear approximation is a function of the power spectrum of the excitation and also a function of its amplitude distribution. Normally distributed noise results in a different FRF than uniformly or binary distributed noise, even if their power spectrum is the same.

This paper considers the behaviour of a mechanical system with nonlinear friction for random multisine excitations. This is a periodic random excitation with a user defined choice for the amplitude spectrum. All the results can easily be generalized to periodic random signals (random amplitude and random phase), at a price of adding an additional expectation with respect to the amplitudes to the expressions as is shortly commented in [5].

A signal $u(t)$ is a random multisine if

$$u(t) = \sum_l A(l) \cos(2\pi(l\Delta f)t + \phi_l), \quad (6)$$

with $A(l)$ the amplitude spectrum, Δf the frequency resolution of the excitation signal and the phases ϕ_l a realization of an independent uniformly distributed random process on $[0, 2\pi]$.

An odd random multisine excitation has nonzero amplitudes $A(l)$ only at the odd frequency lines $l = 2k + 1$ ($k = 0, 1, 2, \dots$), an odd-odd random multisine excitation has nonzero amplitudes $A(l)$ only at the frequency lines $l = 4k + 1$ ($k = 0, 1, 2, \dots$) and a special odd multisine excitation has nonzero amplitudes only at the frequency lines $l = 8k + 1$ and $l = 8k + 3$ ($k = 0, 1, 2, \dots$). Lines that are excited are called excitation lines, the nonexcited lines are called detection lines.

Schoukens et al. [5] show that for odd-odd and special odd multisine excitations, the output spectrum measured at the even and odd detection lines give an estimate of the level of the even and odd nonlinearities present in the system, respectively. The accuracy of the estimate depends on the type of nonlinearity. Vanhoenacker et al. [8] show for lower order nonlinearities (e.g. cubic nonlinearities), that the odd-odd and the special odd multisine excitation can yield significant errors in the estimation of the levels of the systematic and stochastic odd nonlinearities at the excitation lines. They present a more reliable alternative way to determine the detection lines, based on a randomized grid.

This paper investigates the application of this detection method on a mechanical systems with nonlinear friction for odd-odd and special odd excitation.

4 Description of the simulation setup

Figure 2 shows the setup for the simulations. It consists of a mass m connected with a spring k to the ground. The input of the model is the force F acting

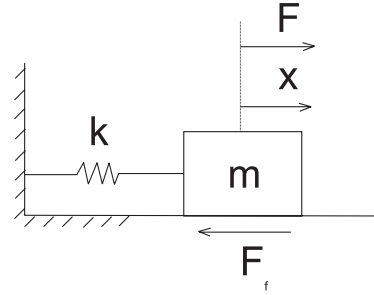


Figure 2: *Simulation setup*

on the mass and the output is the position x of the mass. The dynamic equation is:

$$m \frac{d^2 x}{dt^2} + kx = F - F_f.$$

The friction force F_f between the ground and the mass is calculated by means of the model explained in section 2. Table 1 gives the values of the parameters used in the simulation. The excitation forces are random multisines with a flat amplitude spectrum. Three levels of excitation are considered:

- level 1: a level of excitation which yields a motion which covers the total presliding regime without passing into sliding regime.
- level 2: a level of excitation which yields a motion which covers a small part of the total presliding regime. The excitation signal is ten times smaller as in level 1.
- level 3: a level of excitation which yields a motion which covers the presliding regime and passes into the sliding regime. The excitation signal is ten times larger as in level 1.

parameter	value	units
F_s	1	N
F_c	0.7	N
v_s	0.01	m/s
δ	2	-
σ_1	13	Ns/m
σ_2	0.4	Ns/m
k	80000	N/m
m	1	kg
Δf	0.25	Hz

Table 1: *The parameters used in the simulation setup.*

In the simulations no noise is taken into account. This means that N_G in equation (4) is equal to zero.

5 Results

This section discusses the simulation results obtained for the setup described in section 4. Section 5.1 explains the characteristics of the FRFs obtained using odd multisine excitation and investigates the level of even nonlinearities for the considered mechanical system. Section 5.2 discusses the above mentioned method to detect the odd nonlinearities in the system using odd-odd and special odd multisine excitation.

5.1 Odd multisine excitation

In the simulation experiments, 100 different random odd multisine excitations are applied to the system. For each excitation one period of the steady state response is transferred to the frequency domain and an estimate of the FRF is calculated with the MLE estimator [6]. The resulting FRF is obtained by averaging the individual FRF estimates for the different excitations. The average FRF exists only on the excitation lines).

Figure 3 shows the friction force as a function of the position for one period of a level 1 odd multisine excitation (equation (6) with $k = 5, 7, \dots, 573$). This is an excitation with a bandwidth from 1 Hz to 140 Hz. The excitation is chosen in order to keep the system in the presliding regime. Consequently the hysteresis force will be dominant in the friction force (see figure 3).

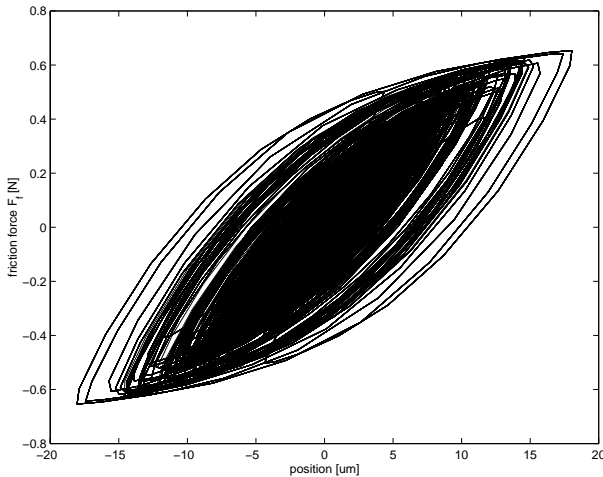


Figure 3: The friction force as a function of the position for one period on an odd excitation.

Figure 4 shows the average FRFs obtained with the three different levels of excitation proposed in section 4. The solid line shows the average FRF for level 1 excitation, the dashed line for level 2 excitation

and the dotted line for level 3 excitation. The three FRFs show a dominant second order behaviour. For the first two levels, the resonance frequency (59 Hz) is approximately equal to $\sqrt{\frac{k+K}{m}}$ with K equal to the average slope of the hysteresis function. K corresponds to the average stiffness of the nonlinear spring characteristic of the asperity junctions. The third FRF shows a shift of the resonance peak to the left. The resonance frequency (45 Hz) is equal to $\sqrt{\frac{k}{m}}$, i.e. it does not depend on K due to the fact that for the third case the system does not stay in the presliding regime but goes to the sliding regime (the maximum value of F is larger than F_s) and the asperity junctions, acting as a nonlinear spring in presliding, are broken.

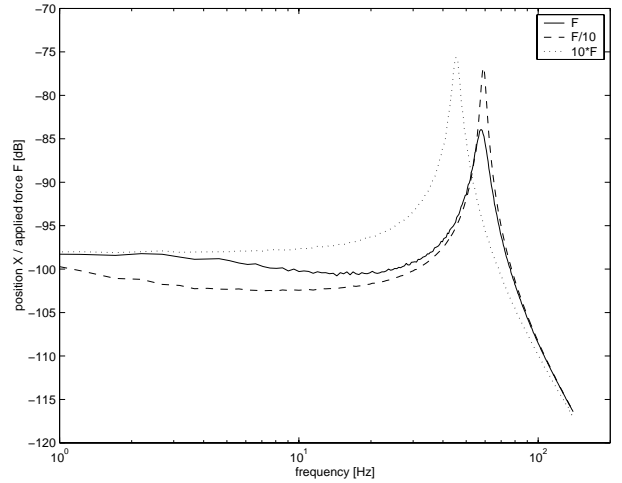


Figure 4: The average FRFs for different amplitudes of the excitation signal F .

Inspection of the frequency contents of the response at detection lines allows us to investigate the presence of even nonlinearities. The output spectrum at the excitation lines are determined from:

$$\frac{E[Y_k U_k^*]}{|U_k|}. \quad (7)$$

$E[.]$ represents the expected value. The stochastic contributions at the excitation lines can be estimated as follows:

$$\frac{\sigma(Y_k U_k^*)}{|U_k|}. \quad (8)$$

$\sigma(.)$ represents the standard deviation. The stochastic contributions at the detection lines can be estimated by taking the root mean square (RMS) of the output:

$$\sqrt{\frac{|Y_{k_1}|^2 + |Y_{k_2}|^2 + \dots + |Y_{k_{100}}|^2}{100}}, \quad (9)$$

with Y_{k_i} the DFT of the output signal at frequency k of the i^{th} excitation.

Figure 5 shows the output spectrum for the odd multisine excitation. The solid line shows the spectrum at the excitation lines, the dashed line shows the stochastic contribution at the detection lines and the dotted line is the stochastic contribution at the excitation lines.

The stochastic contribution at the detection lines is approximately 100 dB less than the stochastic contribution at the excitation lines. Only the even nonlinearities excite the even harmonics at the output ($2k$, $k = 1, 2, \dots$), while the odd nonlinearities appear only at the odd harmonics ($2k + 1$, $k = 1, 2, \dots$) [5]. Thus the system used here has no even nonlinearities, which can be explained by the point symmetric property of the friction model.

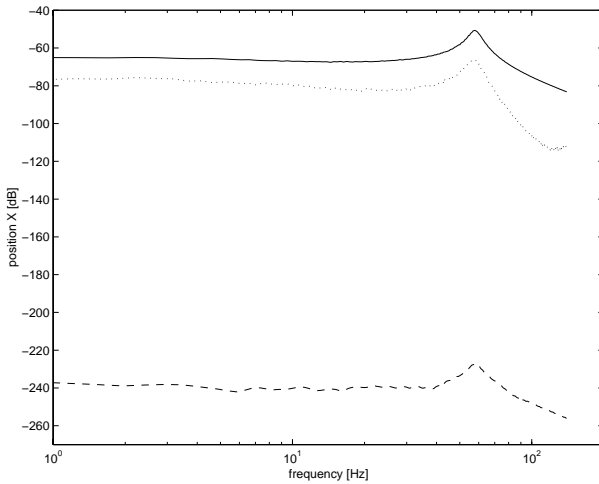


Figure 5: The spectrum of the output signal (the position) with an odd multisine excitation. In solid line the spectrum at the excitation lines and in dashed and dotted lines the spectra of the stochastic contributions at the detection and excitation lines respectively.

5.2 Odd-odd multisine and special odd multisine excitation

The basic idea of this simulation is to excite the system with an odd-odd multisine, where only the frequencies $4k + 1$, $k = 2, \dots, k_{max}$ in equation (6) have amplitudes different from zero, and with an special odd multisine [9, 8], where only the frequencies $8k + 1$ and $8k + 3$, $k = 1, 2, 3, \dots, k_{max}$ in equation (6) have amplitudes different from zero.

Due to the choice of the excitation signal we get the following possibilities:

for the odd-odd multisine

- at lines $4k + 1$ (the excitation lines): the output consists of the linear contribution + odd systematic and stochastic nonlinear distortions,
- at lines $4k + 2$ (the even detection lines): only the even stochastic nonlinear distortions appear,
- at lines $4k + 3$ (the odd detection lines): only odd stochastic nonlinear distortions appear,

for the special odd multisine

- at lines $8k + 1$ and $8k + 3$ (the excitation lines): the output consists of the linear contribution + odd systematic and stochastic nonlinear distortions,
- at even lines (the even detection lines): only the even stochastic nonlinear distortions appear,
- at lines $8k + 5$ and $8k + 7$ (the odd detection lines): only odd stochastic nonlinear distortions appear.

Figure 6 shows the average FRFs and their standard deviation resulting from odd multisine excitation (solid line), from odd-odd multisine excitation (dashed line) and from special odd multisine excitation (dotted line). The stars indicate the difference between the average FRFs resulting from odd-odd and special odd multisine excitation, on the common frequency lines. The difference is of the same order of magnitude as the standard deviation on these FRFs, which shows that the systematic contribution of the nonlinearities is independent of the type of multisine excitation.

The distortions due to the friction force on the linear behaviour of the mechanical system can be analyzed at the spectrum of the output signal. The results for the odd-odd and the special odd excitations, level 1, are given in respectively solid and dashed line in figure 7. Curves *a* show the average output spectra at the excitation lines calculated using equation (7). Curves *b* show the stochastic contributions at the excitation lines calculated using equation (8). The curves *c* give the stochastic contributions at the detection lines calculated using equation (9). The output spectrum at the even detection lines are not shown: they are, similar to the case of odd excitation, 100 dB less than the stochastic contribution at the excitation lines.

The output average spectra (curves *a*) and the stochastic distortions at the excitation lines (curves *b*)

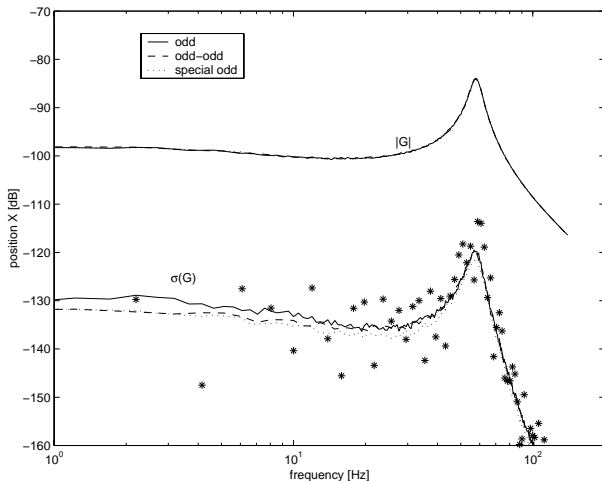


Figure 6: The average FRFs and their standard deviation resulting from odd multisine excitation (solid line), from odd-odd multisine excitation (dashed line) and from special odd multisine excitation (dotted line). The stars indicate the difference between the average FRFs resulting from odd-odd and special odd multisine excitation, on the common frequency lines.

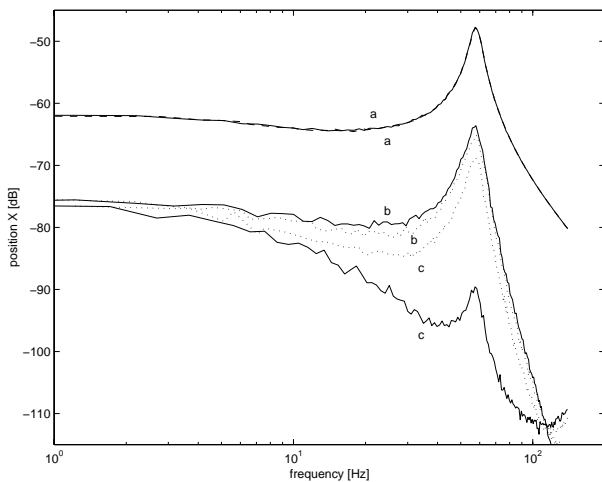


Figure 7: Curves *a* show the mean of the amplitudes of the output spectrum at the excitation lines, curves *b* show the standard deviation on these and curves *c* show the root mean squares of the amplitudes of the output spectrum at the odd detection lines. The results for odd-odd excitation are shown in solid lines, the results for special odd excitation are shown in dotted lines.

are approximately the same for the two types of excitation. Curves *c* show the RMS of the amplitude of the output spectra at the odd detection lines. Figure 7 shows a significant difference between these curves for the two excitations. Schoukens et al. [5] show that the output at the odd detection lines resulting from

one single odd-odd or special odd multisine excitation can be used as an estimate of the stochastic odd nonlinearities. Vanhoenacker et al. [8] show that this estimate can have a significant bias, which is in this case approximately 20 dB at the resonance frequency. The special odd excitation yields a better estimate of the stochastic nonlinear contributions. This estimate is approximately equal to the stochastic nonlinear contributions at the excitation lines (curve *b*). This corresponds to the results presented in [8]. Special odd multisine excitation allows more local combinations of the frequency lines than it is the case for odd-odd multisine excitation, therefore yielding a level of stochastic nonlinear contribution which corresponds more closely to that resulting from a solid multisine excitation. The correspondence between the curves *b* and *c* resulting from the special odd multisine excitation is not perfect and probably corresponds to the error (2 to 3 dB) introduced by this type of excitation as reported in [8].

The stochastic nonlinear contribution at the detection lines for the special odd multisine excitation (curve *c* dotted line) is also a measure for the systematic nonlinear contribution at the excitation lines. [8] shows that the difference is maximum 8 dB. This is the case for a pure third order nonlinearity. In [8] other types of multisines are considered which give a more accurate estimate of the stochastic and the systematic nonlinear contributions.

On a statistical basis (by looking at the averages over 100 excitations), it is shown, that for a mechanical system with friction, the spectrum at the detection lines for a special odd multisine excitation is a reliable estimate for the stochastic and systematic nonlinear contribution. When there is only the possibility to do one experiment, we cannot use the standard deviation on the output spectrum as a measure for the stochastic (and the systematic) nonlinear contribution. By using a special odd multisine excitation, not only a good estimate of the RLDS is available but also an estimate of the nonlinear contribution by looking at the output spectrum at the detection lines.

6 Conclusions

This paper deals with the nonlinear distortions, caused by friction, on FRF measurements on mechanical systems. The nonlinear friction force contains no even nonlinearities. The odd, odd-odd and special odd multisine excitations yield identical linearizations of the system (i.e. RLDS). The special

odd multisine allows to estimate the level of stochastic and systematic nonlinearity contributions by looking at the output spectrum at the detection lines. The estimate is more reliable than the one resulting from odd-odd multisine excitation which yields a considerable bias. Therefore if one can perform only one excitation, the special odd multisine is the preferred excitation signal for mechanical systems with friction.

Acknowledgement

This text presents research results of the Belgian programme on Interuniversity Poles of attraction initiated by the Belgian State, Prime Minister's Office, Science Policy Programming. The scientific responsibility is assumed by its authors.

References

- [1] J.S. Bendat and A.G. Piersol. *Engineering applications of correlation and spectral analysis*. John Wiley & Sons, New York, 1980.
- [2] C. Canudas de Wit, H. Olsson, K. Aström, and P. Lischinsky. A new model for control of systems with friction. *IEEE Transactions on Automatic Control*, 40(5):419–425, 1995.
- [3] P. Eykhoff. *System identification, parameter and state estimation*. New York: John Wiley & Sons, 1974.
- [4] I.D. Mayergoyz. *Mathematical models of hysteresis*. Springer-Verlag, New-York, 1991.
- [5] J. Schoukens, T. Dobrowiecki, and R. Pintelon. Parametric and non-parametric identification of linear systems in the presence of nonlinear distortions. *IEEE Trans. Autom. Control*, AC43(2):176–190, 1998.
- [6] J. Schoukens and R. Pintelon. *Identification of Linear Systems: A Practical Guideline to Accurate Modeling*. London: Pergamon Press, 1991.
- [7] J. Swevers, F. Al-Bender, C. Ganseman, and T. Prajogo. An integrated friction model structure with improved presliding behaviour for accurate friction compensation. *IEEE Transactions on Automatic Control*, accepted for publication, May, 2000.
- [8] K. Vanhoenacker, T. Dobrowiecki, and J. Schoukens. Design of multisine excitations to characterize the nonlinear distortions during frf-measurements. *WISP99 IEEE International Workshop on Intelligent Signal Processing*, 1999.
- [9] K. Vanhoenacker and J. Schoukens. Frequency response function measurements in the presence of nonlinear distortions. *IMTC*, 2000.